KSTLE International Journal, Vol. 2, No. 1, June 2001, pp. 59-64

A Parametric Study on the Characteristics of the Oil-Lubricated Wave Journal Bearing

Hyun-Seung Suh and Yoon-Chul Rhim†

Center for Information Storage Device, Yonsei University, Seoul, Korea

Abstract : A new bearing concept, the wave journal bearing, has been developed to improve the static and dynamic performance of a hydrodynamic journal bearing. This concept features a wave in bearing surface. Not only straight but also twisted wave journal bearings are investigated numerically. The performances of straight and twisted bearings are compared to a plain journal bearing over a wide range of eccentricity. The bearing load and stability characteristics are dependent on the geometric parameters such as the number of waves, the amplitude and the starting point of the wave relative to the applied load direction. The bearing performance is analyzed for various configurations and for both cases of smooth and wave member rotation. The wave journal bearing, especially for the twisted one, offers better stability than the plain journal bearing under all eccentricity ratios and load orientation.

Key words : Wave journal bearing, twisted wave, static and dynamic performance, mumerical study

Introduction

Spindle motor bearings are required high speed and superior vibration characteristics for better performance, miniaturization for compactness, and low cost for economy. Especially, stable rotation of the spindle motor bearing is indispensable to give full play of the sophisticated electro-mechanical device such as, hard disk drive (HDD) for the information storage device. Non-contacting journal bearings have been replaced rolling element bearings to satisfy these various requirements. But plain journal bearings have poor vibration characteristics so that many researchers have been trying to improve the stability characteristics of the journal bearing by adding holes, lobes, spirals, and herringbone-grooves on either journal or bearing surface.

In 1990's, new bearing concept, the wave journal bearing, was developed to improve the static and dynamic performances of the plain journal bearing. Mokhar *et al.* [1] analyzed the static characteristics of the journal bearing with undulating surfaces. Dimofte [2,3] proposed the concept of the wave journal bearing and studied on the characteristics of it with compressible fluid. Walker [4] *et al.* conducted experiments of air-lubricated wave journal bearing and concluded that the stability of the wave journal bearing was superior than that of the plain journal bearing. In this study, we present numerical analysis of the oil-lubricated wave journal bearing with various geometric parameters for the cases of smooth and wave member rotating as well as for the cases of straight and twisted wave in axial direction.

†Corresponding author; Tel: 82-2-2123-2820; Fax: 82-2-312-2159
E-mail: rhimyc@yonsei.ac.kr

Analysis

A schematic geometry of three-wave journal bearing is shown in Fig. 1. The variation in fluid film thickness along the circumference can be defined as follows:

$$h = h_{plain} + h_{wave} = c + e\cos\theta + e_w\cos[n_w(\theta + \alpha)] \quad (1)$$

where c is the radial clearance which is defined as the difference between the mean circle radius of the wave and that of the journal, e, e_w and n_w represent the eccentricity, the wave amplitude, and the number of waves, respectively. The angle a is the angle between the starting point of the wave and the line of centers and θ is the angular coordinate starting from the line of centers in counter-clockwise as shown in Fig. 1. The wave position angle γ is the angle between the starting point of the wave and the direction of the applied load. The wave amplitude is expressed as the wave amplitude ratio, ε_w (e_w/c) which is normalized with the clearance, c.

The fluid film thickness of the twisted wave journal bearing can be obtained by shifting the fluid film thickness of the wave

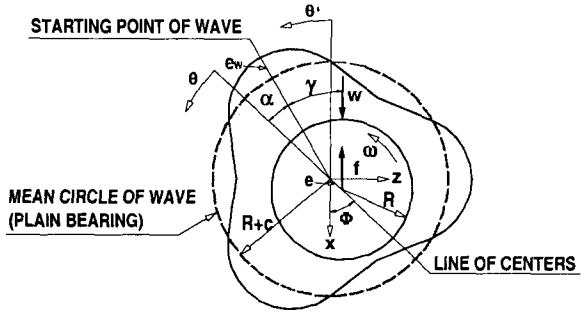

Fig. 1. Three-wave and plain journal bearing geometry.

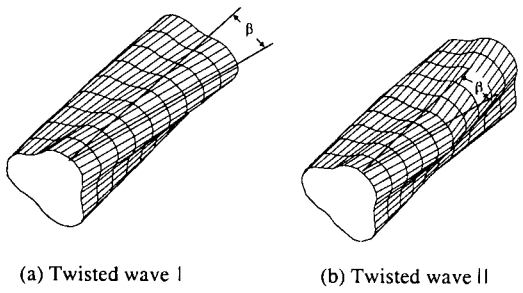

(a) Twisted wave I (b) Twisted wave II

Fig. 2. Twisted wave journal bearing geometry.

journal bearing in circumferential direction along the axis. Then the rates of the change in film thickness both for circumferential and axial directions can be obtained numerically. Figure 2 shows two kinds of the twisted wave journal bearings. One is twisted in one direction along the axis, the other is twisted as chevron shape. The twisted angle β is defined as shown in Fig. 2.

Neglecting the inertia effect of the fluid, the appropriate Reynolds equation usually used for thin fluid film geometry is:

$$\frac{1}{R^2}\frac{\partial}{\partial\theta}\left(\frac{h^3}{12\mu_o}\frac{\partial p}{\partial\theta}\right)+\frac{\partial}{\partial y}\left(\frac{h^3}{12\mu_o}\frac{\partial p}{\partial y}\right)=\frac{\omega}{2}\frac{\partial h}{\partial\theta}+\frac{\partial h}{\partial t} \tag{2}$$

where R is the journal radius, ω is the journal angular speed, and μ_o is the oil viscosity. The stiffness and damping coefficients of the bearing can be obtained by means of perturbation method considering small journal perturbations (Δx, Δz) about steady-state journal position. [5] The film thickness and the pressure are assumed to be as follows:

$$\begin{aligned} h &= h_o + \Delta x\cos\theta' + \Delta z\sin\theta' \\ p &= p_o + p_x\Delta x + p_z\Delta z + p'_x\Delta\ddot{x} + p'_z\Delta\ddot{z} \end{aligned} \tag{3}$$

where h_o denotes the film thickness for steady-state, and

$$\begin{aligned} p_o &= (p)_o \\ p_x &= \left(\frac{\partial p}{\partial x}\right)_o, \qquad p_z = \left(\frac{\partial p}{\partial z}\right)_o \\ p'_x &= \left(\frac{\partial p}{\partial\ddot{x}}\right)_o, \qquad p'_z = \left(\frac{\partial p}{\partial\ddot{z}}\right)_o \end{aligned} \tag{4}$$

Substitution of the Eqn. (3) into the Reynolds equation (1) gives a set of differential equation of pressure:

$$\left[\frac{1}{R^2}\frac{\partial}{\partial\theta'}\left(\frac{h_o^3}{12\mu_o}\frac{\partial}{\partial\theta'}\right)+\frac{\partial}{\partial y}\left(\frac{h_o^3}{12\mu_o}\frac{\partial}{\partial y}\right)\right]\begin{Bmatrix} p_o \\ p_x \\ p_z \\ p'_x \\ p'_z \end{Bmatrix}$$

$$= \begin{Bmatrix} \dfrac{\omega}{2}\dfrac{\partial h_o}{\partial\theta'} \\ -\dfrac{\omega}{2}\left(\sin\theta' + \dfrac{3\cos\theta'}{h_o}\dfrac{\partial h_o}{\partial\theta'}\right) - \dfrac{h_o^3}{4\mu_o}\left[\dfrac{1}{R^2}\dfrac{\partial p_0}{\partial\theta'}\dfrac{\partial}{\partial\theta'}\left(\dfrac{\cos\theta'}{h_o}\right)+\dfrac{\partial p_o}{\partial y}\dfrac{\partial}{\partial y}\left(\dfrac{\cos\theta'}{h_o}\right)\right] \\ \dfrac{\omega}{2}\left(\cos\theta' - \dfrac{3\sin\theta'}{h_o}\dfrac{\partial h_o}{\partial\theta'}\right) - \dfrac{h_o^3}{4\mu_o}\left[\dfrac{1}{R^2}\dfrac{\partial p_0}{\partial\theta'}\dfrac{\partial}{\partial\theta'}\left(\dfrac{\sin\theta'}{h_o}\right)+\dfrac{\partial p_o}{\partial y}\dfrac{\partial}{\partial y}\left(\dfrac{\sin\theta'}{h_o}\right)\right] \\ \cos\theta' \\ \sin\theta' \end{Bmatrix} \tag{5}$$

In order to analyze the effect of twisted wave, the rate of change of the film thickness in axial direction, $\partial h_o/\partial y$, should be included into Eqn. (5). The boundary conditions for Eqn. (5) are as follows:

$$\begin{aligned} p_o &= p_a \\ p_x &= p_z + p'_x + p'_z = 0 \end{aligned} \tag{6}$$

at both ends of the bearing in axial direction and

$$\frac{\partial p_o}{\partial\theta} = 0, \quad p_o = p_a, \tag{7}$$

along the cavitation boundary, where p_a represents the ambient pressure. Periodic condition is used for the circumferential direction.

The resultant reaction load is decomposed into f_x and f_z in x and z directions, respectively:

$$\begin{Bmatrix} f_x \\ f_z \end{Bmatrix} = \begin{Bmatrix} (f_x)_o \\ (f_z)_o \end{Bmatrix} + \begin{pmatrix} k_{xx} & k_{xz} \\ k_{zx} & k_{zz} \end{pmatrix}\begin{Bmatrix} \Delta x \\ \Delta z \end{Bmatrix} + \begin{pmatrix} b_{xx} & b_{xz} \\ b_{zx} & b_{zz} \end{pmatrix}\begin{Bmatrix} \Delta\ddot{x} \\ \Delta\ddot{z} \end{Bmatrix} \tag{8}$$

where

$$\begin{aligned} k_{xx} &= \left(\frac{\partial f_x}{\partial x}\right)_o, \quad k_{xz} = \left(\frac{\partial f_x}{\partial z}\right)_o, \quad k_{zx} = \left(\frac{\partial f_z}{\partial x}\right)_o, \quad k_{zz} = \left(\frac{\partial f_z}{\partial z}\right)_o \\ b_{xx} &= \left(\frac{\partial f_x}{\partial\ddot{x}}\right)_o, \quad b_{xz} = \left(\frac{\partial f_x}{\partial\ddot{z}}\right)_o, \quad b_{zx} = \left(\frac{\partial f_z}{\partial\ddot{x}}\right)_o, \quad b_{zz} = \left(\frac{\partial f_z}{\partial\ddot{z}}\right)_o \end{aligned} \tag{9}$$

The finite difference method is applied to Eqn. (5) and the alternating direction implicit method is used to compute pressure iteratively. The iteration repeats until the relative error of the pressure at every points is less than 10^{-7}. Reynolds boundary condition is applied at every iterations. Integration of the pressure distribution over the journal surface gives the reaction forces and resultant attitude angle of the fluid film bearing and then the stiffness and damping coefficient, k and b can be calculated.

The stability analysis is followed once the dynamic coefficients of the bearing are obtained. Equations of motion for the constant speed journal of mass m_a are:

$$\begin{aligned} m_a\Delta\ddot{x} &= f_x \\ m_a\Delta\ddot{z} &= f_z \end{aligned} \tag{10}$$

Equation (10) is recast for the given coordinate system as follows:

$$\begin{pmatrix} m_a & 0 \\ 0 & m_a \end{pmatrix}\begin{Bmatrix} \Delta\ddot{x} \\ \Delta\ddot{z} \end{Bmatrix} + \begin{pmatrix} c_{xx} & c_{xz} \\ c_{zx} & c_{zz} \end{pmatrix}\begin{Bmatrix} \Delta\dot{x} \\ \Delta\dot{z} \end{Bmatrix} + \begin{pmatrix} k_{xx} & k_{xz} \\ k_{zx} & k_{zz} \end{pmatrix}\begin{Bmatrix} \Delta x \\ \Delta z \end{Bmatrix} = \begin{Bmatrix} 0 \\ 0 \end{Bmatrix} \tag{11}$$

The solution to Eqn. (11) is of the type:

$$\begin{Bmatrix} \Delta x \\ \Delta z \end{Bmatrix} = \begin{Bmatrix} x_h \\ z_h \end{Bmatrix} e^{\Omega t} \tag{12}$$

where $\Omega = -\Omega_d + i\Omega_v$. Substituting Eqn. (12) into Eqn. (11) gives:

$$\begin{pmatrix} \bar{\Omega}^2 M_a + \bar{\Omega}B_{xx} + K_{xx} & \bar{\Omega}B_{xz} + K_{xz} \\ \bar{\Omega}B_{zx} + K_{zx} & \bar{\Omega}^2 M_a + \bar{\Omega}B_{zz} + K_{zz} \end{pmatrix}\begin{Bmatrix} x_h \\ z_h \end{Bmatrix} e^{\bar{\Omega}\omega t} = \begin{Bmatrix} 0 \\ 0 \end{Bmatrix} \tag{13}$$

where

$$\bar{\Omega} = \frac{\Omega}{\omega} \quad M_a = \frac{cm_a\omega^2}{p_a LD} \tag{14}$$

$$\begin{pmatrix} K_{xx} & K_{xz} \\ K_{zx} & K_{zz} \end{pmatrix} = \frac{c}{p_a LD}\begin{pmatrix} k_{xx} & k_{xz} \\ k_{zx} & k_{zz} \end{pmatrix}$$

$$\begin{pmatrix} B_{xx} & B_{xz} \\ B_{zx} & B_{zz} \end{pmatrix} = \frac{c\omega}{p_a LD}\begin{pmatrix} b_{xx} & b_{xz} \\ b_{zx} & b_{zz} \end{pmatrix}$$

D and L represent the journal diameter and the bearing length, respectively. The instability of the bearing occurs at $\Omega_d = 0$, and the dimensionless critical mass parameter $(M_a)_{cr}$ can be calculated from Eqn. (13):

$$(M_a)_{cr} = \left(\frac{cm_a\omega^2}{p_a LD}\right)_{cr} \tag{15}$$

Results and Discussions

All the results shown in this work is for the case of L/D = 1 for simplicity. The pressure distribution is mainly affected by the waves as can be seen in Fig. 3, which differs significantly from the plain journal bearing. The wave journal bearing generates pressure even at zero eccentricity so that it can obtain the high stiffness and stability performance even the bearing is operated near the concentric position. The pressure distribution is plotted in Fig. 3 using a dimensionless pressure, P_o, and the load carrying capacity, which can be obtained by integration of the pressure distribution over the bearing surface, is normalized as follows:

$$P_o = \frac{p_o}{p_a}, \quad F = \frac{f}{p_a LD} \tag{16}$$

The same eccentricity ratio of 0.2 was set in computer program to compare the load carrying capacity of the wave journal bearing to the plain journal bearing. The load carrying capacity of the wave journal bearing depends on the parameters such as eccentricity, the number of waves, the wave amplitude ratio and the wave position angle. As an example, the variation of load carrying capacity for the wave amplitude ratio is plotted with respect to the wave posion angle in Fig. 4. As the wave amplitude ratio becomes larger, the load carrying capacity increases more. Furthermore the maximum load can be obtained at certain wave position angle and in reverse, load carrying capacity of wave journal bearing may fall below that of plain journal bearing for certain wave position angle. That is, the waves position angle must be carefully selected. However, the large wave amplitude ratio can cover up above mentioned problem.

The wave position angle for the maximum load carrying capacity of the 3-wave journal bearing can be decided from the Fig. 4 at each wave amplitude ratio and this corresponds to $\alpha = 0$. Among the attitude angle, the wave position angle and the angle between the starting point of the wave and the line of centers (a), the following relation, which is shown in Fig. 1, can be written:

$$\gamma = \Phi - \alpha \tag{17}$$

The wave position angle must be equal to the attitude angle to maximize the effect of wave on load carrying capacity of the 3-wave journal bearing. The attitude angle *vs.* the eccentricity ratio of 3-wave journal bearing when $\alpha = 0$ is plotted in Fig. 5. As the wave amplitude ratio becomes larger, the attitude angle

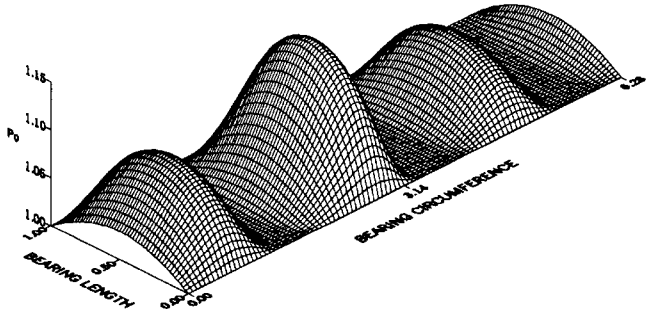

Fig. 3. Pressure distribution of the 3-wave bearing (ε=0.1, ε_w=0.2, α=0, smooth member rotating).

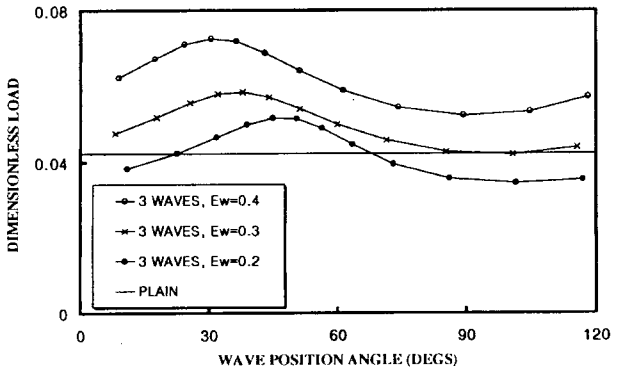

Fig. 4. Dimensionless load vs. wave position angle of 3-wave and plain journal bearing for various wave amplitude ratios (ε=0.2, smooth member rotating).

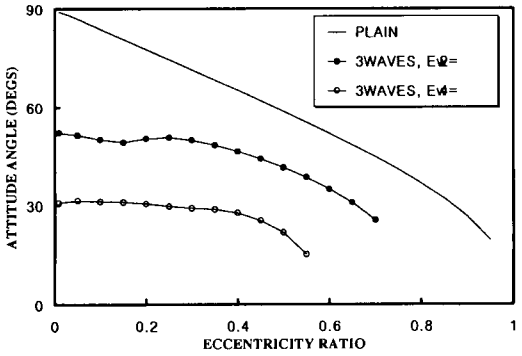

Fig. 5. Attitude angle vs. eccentricity ratio of 3-wave and a plain bearing for various wave amplitude ratio (α=0, smooth member rotating).

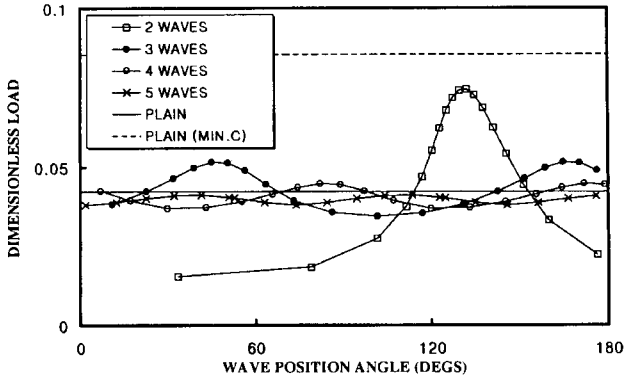

Fig. 6. Dimensionless load vs. wave position angle of wave and plain journal bearing for various number of waves (ε=0.2, ε_w=0.2, smooth member rotating).

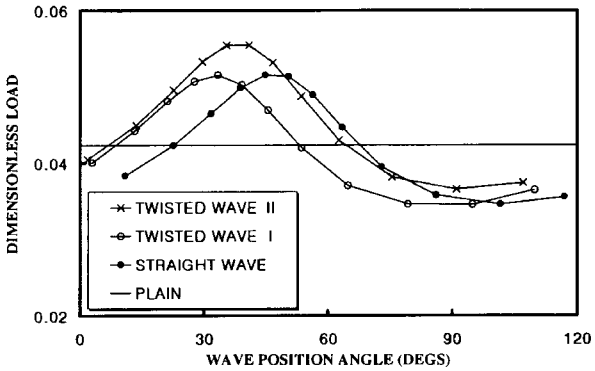

Fig. 7. Dimensionless load vs. wave posotion angle of straight, twisted-wave I and II (3 waves, ε=0.2, ε_w=0.2, smooth member rotating).

at given eccentricity ratio decreases.

To illustrate the effect of the number of waves, the load carrying capacities of wave journal bearings are plotted with respect to the wave position angle for various number of waves in Fig. 6. As the number of waves increases, the load carrying capacity of the wave journal bearing becomes nearly constant regardless of the applied load direction while the maximum value decreases compared to the less number of waves. The dotted line corresponds to the load carrying capacity of the plain journal bearing for the minimum film thickness due to the wave.

The load carrying capacity of the wave journal bearing which is twisted in one direction along the axis (twisted-wave I) and in chevron shape (twisted-wave II) are plotted in Fig. 7, where the eccentricity ratio and the wave amplitude ratio are set to 0.2 and the twisted angle is set to 27.6° at each case. The twisted-wave I has less maximum load carrying capacity compared to the straight-wave journal bearing. On the other hand, the twisted-wave II has more improved maximum load carrying capacity than that of the straight-wave journal bearing.

Figure 8 shows the effect of the twisted angle on the load carrying capacity and the attitude angle of the twisted-wave I and II. As the twisted angle increases, the load carrying capacity and attitude angle of the twisted-wave I and the attitude angle of the twisted-wave II decrease. But the load carrying capacity of the twisted-wave II increases to some extent as if there is an optimal value in twisted angle just like a herringbone groove journal bearing.

When waves are formed on the rotating surface, the film thickness varies with the journal angular position, which makes reaction forces in fluid film vary with time with a fundamental period equal to $(2\pi/\omega)n_w$. The transient characteristics of the wave journal bearing have to be analyzed when the wave member rotates.

Figure 9 shows the dimensionless radial and tangential forces variations of the 3-wave journal bearing with respect to the journal eccentricities. Due to large pressure change in wave by wave, these transient force variations are more prominent for the wave journal bearing with a small number of waves operating at large journal eccentricity.

The bearing stability is illustrated with the dimensionless critical mass parameter defined by Eqn. (15). Figure 10 shows the dimensionless critical mass parameter variations with respect to the wave position angle of 3-wave journal bearing for various wave amplitude ratios. The maximum bearing stability can be obtained with proper selection of the wave position angle, that is, $\alpha = 0$ which is similar to the case for the load carrying capacity. However, wave journal bearing is more stable than plain journal bearing regardless of the wave

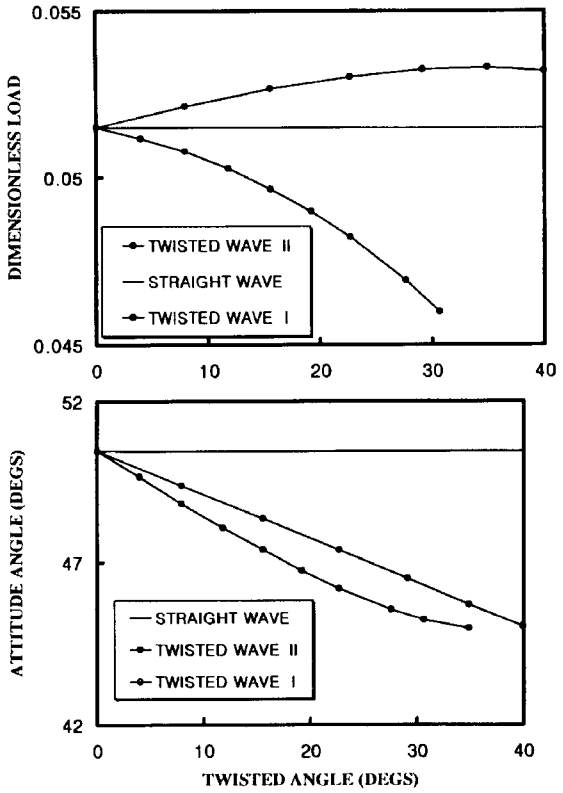

Fig. 8. Dimensionless load capacity and attitude angle vs. twisted angle of straight, twisted-wave I and II (3 waves, ε=0.2, ε_w=0.2, smooth member rotating).

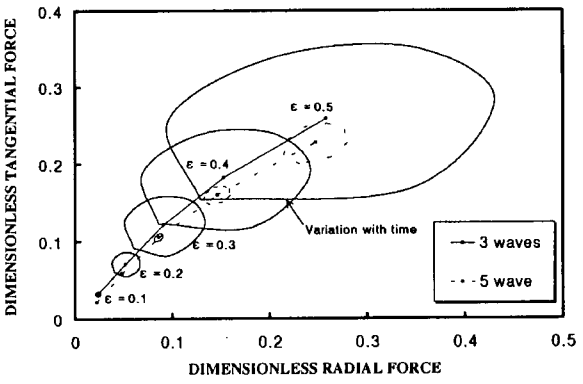

Fig. 9. Time variations of dimensionless tangential force vs. radial force of wave journal bearing, increasing static journal eccentricity (ε_w=0.2, wave member rotating).

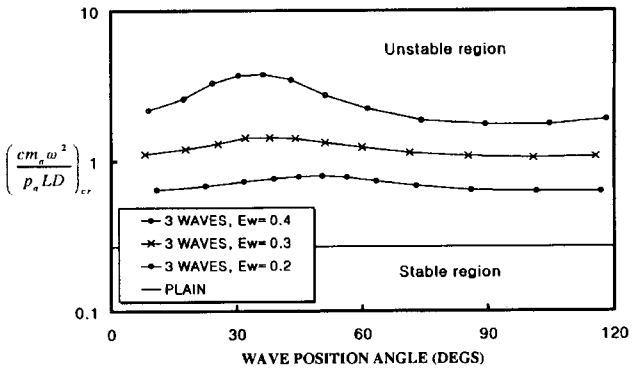

Fig. 10. Dimensionless critical mass parameter vs. wave position angle of 3-wave and plain journal bearing for various wave amplitude ratios (ε=0.2, smooth member rotating).

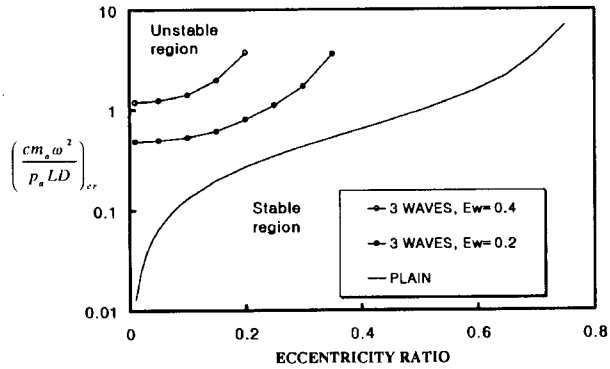

Fig. 11. Dimensionless critical mass parameter vs. eccentricity ratio of 3-wave and plain journal bearing for various wave amplitude ratios (α=0, smooth member rotating).

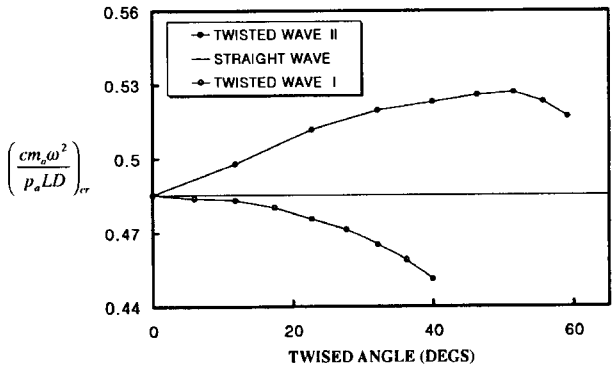

Fig. 12. Dimensionless critical mass parameter vs. twisted angle of straight, twisted-wave and (3 waves, ε=0.01, ε_w=0.2, smooth member rotating).

position angle and better stability is obtained as the wave amplitude ratio increases.

Figure 11 shows the stability map of the 3-wave journal bearing with respect to various wave amplitude ratios for the case of $\alpha = 0$. The wave journal bearing is more stable than the plain journal bearing in all eccentricity range and its difference becomes larger especially near the concentric position where plain journal bearing is easy to become unstable.

The variations of the dimensionless critical mass *vs.* the twisted angle are plotted for the case of the twisted-wave I and II in Fig. 12. The eccentricity ratio of 0.01 was selected because the instability occurs easily near a concentric position. The stability of the twisted-wave II increases as the twisted angle increases to some extent while the stability of the twisted-wave I decreases with the increasing twisted angle. That is, the twisted wave I has poor stability characteristics than even straight wave journal bearing. However, twisted wave I can pump the lubricant into axial direction, that can be applied to improve another characteristics of the spindle motor bearing system.

Conclusions

The characteristics of the wave journal bearing using incompressible lubricant have been analyzed and compared to those of the plain journal bearing. Also the static and dynamic performances of the journal bearing with various wave parameters are investigated numerically. The following conclusions are drawn:

1. By adding the wave geometry on the bearing surface, the load carrying capacity increases as the wave amplitude increases and the static and dynamic performances of the journal bearing are improved.
2. For the case of the smooth member rotating, the position of the wave relative to the applied load gives big influences on the bearing characteristics.
3. As the number of waves increases, the load carrying capacity of the wave journal bearing becomes nearly constant regardless of the direction of the applied load and the maximum value decreases compared to less number of waves.
4. For the wave journal bearing twisted in one direction, the maximum load carrying capacity and the stability decreases as the twisted angle increases. On the other hand, the wave journal bearing twisted in chevron shape has better characteristics in both the load carrying capacity and stability than the straight wave journal bearing.
5. For the case of wave member rotating, the transient force variation increases as the journal eccentricity increases and the number of waves decreases.

Acknowledgment

This work was funded by the Korea Science and Engineering Foundation (KOSEF) through the Center for Information Storage Device(CISD) Grant No. 2000G0201.

References

1. Mokhtar, M. O. A., Aly, W. Y. and Shawki, G. S. A. Computer-Aided Study of Journal Bearings With Undulating Surfaces, ASME Trans. Vol. 106, pp. 468-472, 1984.
2. Dimofte, F., Wave Journal Bearing with Compressible Lubricant-Part: The Wave Bearing Concept and a Comparison to the Circular Bearing, STLE Tribology Trans., Vol. 38, pp. 153-160, 1995.
3. Dimofte, F., Wave Journal Bearing with Compressible Lubricant-Part: A Comparison of the Wave Bearing with a Wave-Groove Bearing and a Lobe Bearing, STLE Tribology Trans., Vol. 38, pp. 364-372, 1995.
4. Walker, J., Dimofte, F. and Addy Jr., H. E., Wave Journal Bearing: Part-Experimental Pressure Measurements and Fractional Frequency Whirl Threshold for Wave and Plain Journal Bearings, Proceedings of the Energy-Sources Technology Conference and Exhibition, Houston, TX, USA New York, NY, The American Society of Mechanical Engineers, pp. 61-68, 1995.
5. Lund, J. W., Review of the Concept of Dynamic Coefficients for Fluid Film Journal Bearings, ASME, Journal of Tribology, Vol. 109, pp. 37-41, 1987.
6. Kang, K., Rhim, Y. and Sung, K. A Study of the Oil-Lubricated Herringbone-Grooved Journal Bearing-Part: Numerical Analysis, ASME Journal of Tribology, Vol. 118, pp. 906-911, 1996.
7. Bonneau, D. and Absi, J., Analysis of Aerodynamic Journal Bearings with Small Number of Herringbone Grooves by Finite Element Method, ASME trans., Vol. 116, pp. 698-704, 1994.
8. Zirkelback, N. and San Andres, L., Finite Element Analysis of Herringbone Groove Journal Bearings: A Parametric Study, ASME Trans., Vol. 120, pp. 234-240, 1998.